Stability and Control of Dynamical Systems with Applications, D. Liu and P. J. Antsaklis (Eds), Control Engineering Series, Birkhauser Boston, 2003.

Trajectory Sensitivity Theory in Non Linear Dynamical Systems: Some Power System Applications

M. A. Pai and T. B. Nguyen*
Dept of Electrical and Computer Engineering
University of Illinois at Urbana-Champaign

Abstract:

Trajectory sensitivity analysis (TSA) has been applied in control system problems for a long time in such areas as optimization, adaptive control etc. Applications in power systems in conjunction with Lyapunov/transient energy functions first appeared in the 80's. More recently, it has found applications on its own by defining a suitable metric on the trajectory sensitivities with respect to the parameters of interest. In this paper we present the theoretical as well as practical applications of TSA for dynamic security applications in power systems. We also discuss the technique to compute critical values of any parameter that induces stability in the system using trajectory sensitivities.

1. Introduction

Security in power systems became an issue after the Northeast blackout in 1965 [1]. Since then a lot of research has been done investigating both static and dynamic aspects of security. While a lot of success has been achieved on the static front [2], such is not the case with dynamic security. Dynamic security assessment (DSA) in power systems comprises of the following main tasks: contingency selection/screening, security evaluation, contingency ranking, and limit computation. Dynamic simulation has historically been the main tool, and currently in combination with heuristics and some form of learning, it still remains as the tool for DSA in the energy control centers. Intensive research since the 60's in applying Lyapunov's direct method has resulted in useful algorithms in the form of transient energy function (TEF) technique [3-5] and single machine equivalent (SIME) technique [6]. Artificial neural network (ANN) and artificial intelligent (AI) based techniques have also been applied [7, 8]. Of these the TEF and SIME techniques are considered the most promising ones by the research community. In the deregulated environment, the existing transmission system often operates at its limit due to inadequate capacity and multilateral transactions. In addition, power systems must be operated to satisfy the transient stability constraints for a set of contingencies. In these situations, dynamic security assessment plays a crucial role. There exists a need to replace the repetitive nature of the dynamic simulation for DSA by a procedure where complex models can be handled easily in a more direct manner. The aim of on-line DSA is to assess the stability of the system to a set of predefined contingencies. These contingencies are user specified or are chosen automatically through some procedure such as a filtering process. For each contingency if the system is stable, it can also provide a security margin based on the technique used. For

---

* Present address: Energy Science and Technology Directorate, Pacific Northwest National Laboratory, Richland, WA.

instance, if critical clearing time is computed, the t_{cr}-t_{cl} is the margin. On the other hand, if the transient energy function (TEF) is used, then V_{cr}-V_{cl} is the margin. The security margin can be used to provide the operators with guidelines to improve system security while at the same time maintaining economic operation. This is known as security-constrained optimization or preventive rescheduling (See Fig 1). The literature on preventive control is largely tied to the TEF method, namely, to enhance the stability margin as defined by the difference between critical energy V_{cr} and energy at clearing V_{cl}. However, the need for computation of the unstable equilibrium point and the absence of an analytical closed form of the energy function makes it difficult to apply for larger and more complex models of machines.

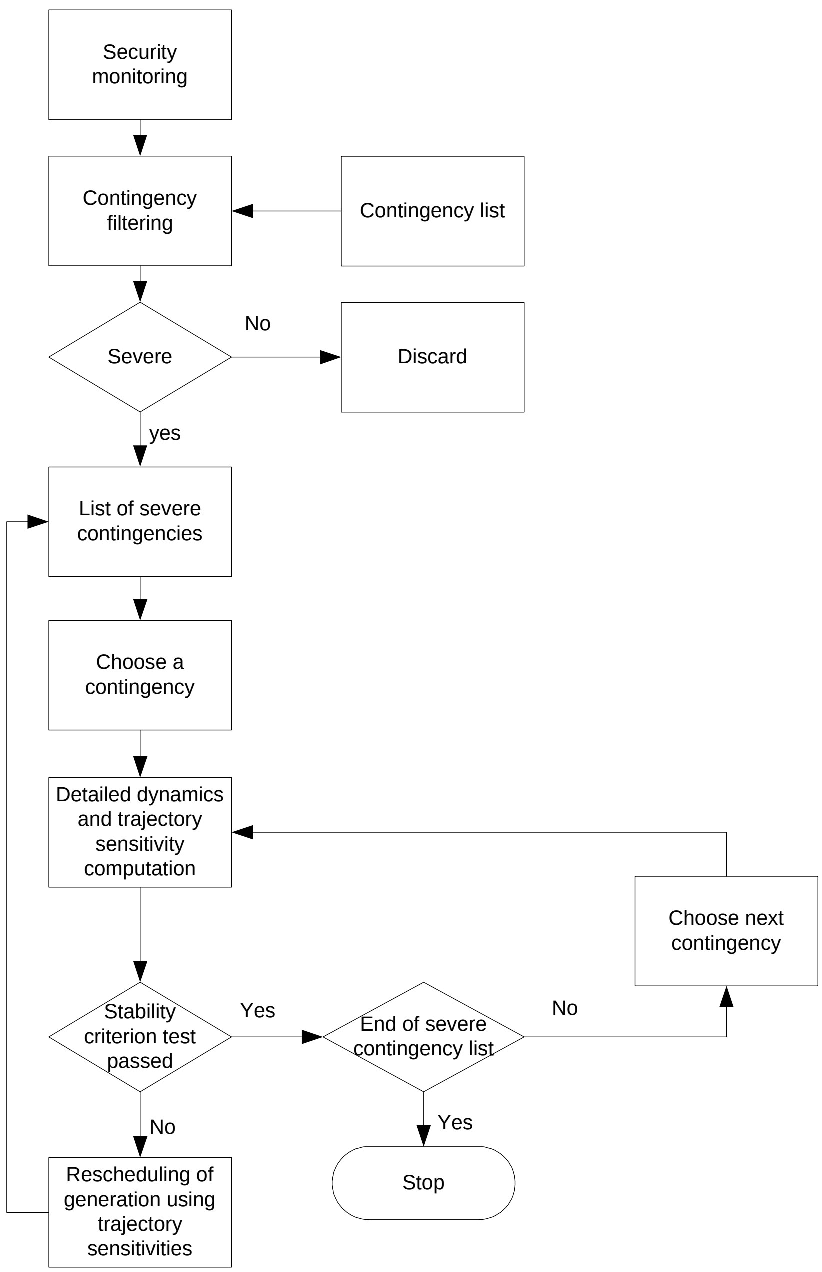

Fig. 1. DSA scheme using trajectory sensitivities

In this paper we review some recent results in applying trajectory sensitivity (TS) techniques [9] to DSA and preventive control. As it will be shown, this new technique has several advantages over all the other techniques:

1. No restriction on complexity of the model.
2. Extension to systems with discrete events is possible.
3. Information other than mere stability can be obtained.
4. Limits to any parameter in the system affecting stability can be studied.
5. Identification of weak links in the transmission network is possible.
6. Preventive strategies can be incorporated easily.

However, the above advantages are obtained at the expense of increased computational cost. This question will also be addressed in this paper. The paper outline is as follows.

In Section 2 we will explain the derivation of the basic theory of trajectory sensitivity analysis (TSA) for differential algebraic equation (DAE) form of the system model. The overall approach to DSA using TSA technique will be explained. In Section 3 we will use the TSA technique to compute critical parameter values such as clearing time, mechanical input power, and line reactance. In Section 4 we will explain the dynamic security constrained dispatch problem and its application [10]. In Section 5 we will use TSA technique to find weak links, vulnerable relays and the electrical centers of the system for a given fault. This information is useful in proper islanding of the system in a self-healing way [11].

2. TRAJECTORY SENSITIVITY ANALYSIS

Sensitivity theory in dynamic systems has a long and rich history well documented in the books by Frank [12] and Eslami [13]. It can be traced back to the work of Bode [14] in designing feedback amplifiers where feedback is used to cancel the effect of unwanted disturbances and parameter variations. The concept of sensitivity matrix using state space analysis can be used [15]. While bulk of the work is in the area of linear time invariant (LTI) systems, the fundamental theory is applicable to nonlinear systems as well. Applications of sensitivity theory or more specifically trajectory sensitivity analysis (TSA) to nonlinear dynamic systems are few. The books of Tomovic [15], Tomovic and Vukobratovic [16], and Cruz [17] contain control-oriented applications.

There have been applications of sensitivity theory to power systems but mostly for linear systems such as eigenvalue sensitivity [18]. From a stability point of view it has been applied for computing sensitivity of the energy margin while using the transient energy function method [3, 4]. Applications of trajectory sensitivity to nonlinear models of power systems are somewhat recent [19].

The application in the linear system arises from the linearization of a nonlinear system around an equilibrium point. Stability of the equilibrium point is evaluated through eigenvalues. In trajectory sensitivity analysis, we linearize around a nominal trajectory and try to interpret the variations around that trajectory. It is a challenge to develop a metric for those variations and relate it to the stability of the nominal trajectory. In [15] the author hints at the intimate connection between trajectory sensitivity analysis and Lyapunov stability but it is not quantified. In this paper we make an attempt to do so.

3. Trajectory Sensitivity Theory for Differential Algebraic Equation (DAE) Model

The development in this section follows Ref [20, 21] where the application to hybrid systems is discussed. A DAE system is a special case of the more general hybrid systems. A fairly accurate description of the power system model is represented by a set of differential algebraic equation of the form

$$\dot{x} = f(x, y, \lambda) \tag{1}$$

$$0 = \begin{cases} g^{-}(x, y, \lambda) & s(x, y, \lambda) < 0 \\ g^{+}(x, y, \lambda) & s(x, y, \lambda) > 0 \end{cases} \tag{2}$$

and a switching occurs when $s(x, y, \lambda) = 0$.

In the above model, x are the dynamic state variables such as machines' rotor angles, velocities, etc.; y are the algebraic variables such as load bus voltage magnitudes and angles; and λ are the system parameters such as line reactances, generator mechanical powers, and fault clearing time. Note that the state variables x are continuous while the algebraic variables y can undergo step changes at the switching instants.

The initial conditions for (1)-(2) are given by

$$x(t_0) = x_0 \quad , \; y(t_0) = y_0$$

where y_0 satisfies $g(x_0, y_0, \lambda) = 0$

For compactness of notation, the following definitions are used

$$\underline{x} = \begin{bmatrix} x \\ \lambda \end{bmatrix}$$

$$\underline{f} = \begin{bmatrix} f \\ 0 \end{bmatrix}$$

With these definitions, (1)-(2) can be written in a compact form as

$$\dot{\underline{x}} = \underline{f}(\underline{x}, y) \tag{3}$$

$$0 = \begin{cases} g^{-}(\underline{x}, y) & s(\underline{x}, y) < 0 \\ g^{+}(\underline{x}, y) & s(\underline{x}, y) > 0 \end{cases} \tag{4}$$

The initial conditions for (1)-(2) are

$$\begin{aligned} \underline{x}(t_0) &= \underline{x}_0 \\ y(t_0) &= y_0 \end{aligned} \tag{5}$$

We divide the time interval as consisting of non-switching subintervals and switching instants for which the sensitivity model is now developed.

Trajectory sensitivity calculation for non-switching periods

This section gives the analytical formulae for calculating sensitivities $\underline{x}_{\underline{x}_0}(t)$ and $y_{\underline{x}_0}(t)$ on the non -switching time intervals as discussed in [21]. On these intervals, the DA systems can be written in the form

$$\dot{\underline{x}} = \underline{f}(\underline{x}, y) \tag{6}$$

$$0 = g(\underline{x}, y) \tag{7}$$

Differentiating (6) and (7) with respect to the initial conditions $\underline{x}_0$ yields

$$\dot{\underline{x}}_{\underline{x}_0} = \underline{f}_{\underline{x}}(t)\underline{x}_{\underline{x}_0} + \underline{f}_y(t) y_{\underline{x}_0} \tag{8}$$

$$0 = g_{\underline{x}}(t)\underline{x}_{\underline{x}_0} + g_y(t) y_{\underline{x}_0} \tag{9}$$

where $\underline{f}_{\underline{x}}$, $\underline{f}_y$, $g_{\underline{x}}$, and g_y are time-varying matrices and are calculated along the system trajectories.

Initial conditions for $\underline{x}_{\underline{x}_0}$ are obtained by differentiating (5) with respect to $\underline{x}_0$ as

$$\underline{x}_{\underline{x}_0}(t_0) = I \tag{10}$$

where I is the identity matrix.

Using (10) and assuming that $g_y(t_0)$ is nonsingular along the trajectories, initial condition for $y_{\underline{x}_0}$ can be calculated from (9) as

$$y_{\underline{x}_0}(t_0) = -[g_y(t_0)]^{-1} g_{\underline{x}}(t_0) \tag{11}$$

Therefore, the trajectory sensitivities can be obtained by solving (6) and (7) simultaneously with (8) and (9) using any numerical method with (5), (10), and (11) as the initial conditions.

At switching instants, it is necessary to calculate the jump conditions that describe the behavior of the trajectory sensitivities at the discontinuities. Since we are considering time instants, which do not depend on the states, the sensitivities of the states will be continuous whereas those of the algebraic are not. When the trajectory sensitivities are known, the perturbed trajectories can be estimated by first-order approximation without redoing simulation as

$$\Delta \underline{x}(t) \approx \underline{x}_{\underline{x}_0}(t)\Delta \underline{x}_0 \tag{12}$$

$$\Delta y(t) \approx y_{\underline{x}_0}(t)\Delta \underline{x}_0 \tag{13}$$

Computation of critical values of parameters using energy function as a metric [22]

In the literature, trajectory sensitivities have been used [4] to compute the energy margin sensitivity with respect to system parameters such as interface line flow, system loading, etc. using TEF methods. In these cases, the critical energy v_{cr}, which is the energy at the controlling u.e.p., depends on the parameters. Therefore, computation of $\dfrac{\partial \nu_{cr}}{\partial t_{cl}}$ is necessary while using the TEF method. This is computationally a difficult task. On the other hand, because the energy function $\nu(x)$ is used here only as a metric to monitor the system sensitivity for different t_{cl}, we can avoid the computation of ν_{cr} and use $\nu(x)$ directly.

The process of estimating critical values of parameters will be illustrated using the clearing time t_{cl}. However, the process is appropriate for any parameter that can induce instability such as mechanical power P_M. We can use the sensitivity $\dfrac{\partial \nu}{\partial t_{cl}}$ to estimate t_{cr} directly. With the classical model for machines, the energy function $\nu(x)$ for a structure-preserving model is computed as follows.

The post fault power system can be represented by the DAE model in the center of angle reference frame as [3]

$$\dot{\theta}_{n_0+i} = \tilde{\omega}_{g_i} \qquad i = 1, \ldots, m \tag{14}$$

$$M_i \dot{\tilde{\omega}}_{g_i} = P_{M_i} - \sum_{j=1}^{n} B_{n_0+i,j} V_{n_0+i} V_j \; \sin\left(\theta_{n_0+i} - \theta_j\right) - \frac{M_i}{M_T} P_{COA} \qquad i = 1, \ldots, m \tag{15}$$

$$P_{d_i} + \sum_{j=1}^{n} B_{ij} V_i V_j \sin(\theta_i - \theta_j) = 0 \qquad i = 1, \ldots, n_0 \tag{16}$$

$$Q_{d_i}(V_i) - \sum_{j=1}^{n} B_{ij} V_i V_j \cos(\theta_i - \theta_j) = 0 \qquad i = 1, \ldots, n_0 \tag{17}$$

where m is the number of machines, n_0 is the number of buses in the system, and

$$P_{COA} = \sum_{i=1}^{m} \left(P_{M_i} - \sum_{j=1}^{n} B_{ij} V_i V_j \sin(\theta_i - \theta_j) \right)$$

We assume constant real power loads and voltage dependent reactive power load as

$$Q_{di}(V_i) = Q_{di}^{s} \left(\frac{V_i}{V_i^{s}} \right)^{\alpha} \tag{18}$$

where Q_i^s and V_i^s are the nominal steady state reactive power load and voltage magnitude at the ith bus, and α is the reactive power load index.

The corresponding energy function is established as [3]

Stability and Control of Dynamical Systems with Applications, D. Liu and P. J. Antsaklis (Eds), Control Engineering Series, Birkhauser Boston, 2003.

$$
\begin{aligned}
\nu(\tilde{\omega}_g,\theta,V) = {} & \frac{1}{2}\sum_{i=1}^{m} M_i \tilde{\omega}_{g_i}^2 - \sum_{i=1}^{m} P_{M_i}(\theta_{n_0+i}-\theta_{n_0+i}^s) + \sum_{i=1}^{n_0} P_{d_i}(\theta_i-\theta_i^s) \\
& -\frac{1}{2}\sum_{i=1}^{n_0} B_{ii}(V_i^2 - V_i^{s2}) + \sum_{i=1}^{n_0}\frac{Q_{d_i}^s}{\alpha V_i^{s\alpha}}(V_i^{\alpha}-V_i^{s\alpha}) \\
& -\sum_{i=1}^{n-1}\sum_{j=i+1}^{n} B_{ij}(V_iV_j\cos\theta_{ij} - V_i^sV_j^s\cos\theta_{ij}^s)
\end{aligned}
\tag{19}
$$

where $\theta_{ij} = \theta_i - \theta_j$.

The sensitivity *S* of the energy function $\nu(x)$ with respect to clearing time ($\lambda = t_{cl}$) is obtained by taking partial derivatives of (19) with respect to t_{cl} as

$$
\begin{aligned}
S = \frac{\partial \nu}{\partial t_{cl}} = {} & \sum_{i=1}^{m} M_i \tilde{\omega}_{g_i}\frac{\partial \tilde{\omega}_{g_i}}{\partial t_{cl}} - \sum_{i=1}^{m} P_{M_i}\frac{\partial \theta_{n_0+i}}{\partial t_{cl}} + \sum_{i=1}^{n_0} P_{d_i}\frac{\partial \theta_i}{\partial t_{cl}} - \sum_{i=1}^{n_0} B_{ii}V_i\frac{\partial V_i}{\partial t_{cl}} \\
& + \sum_{i=1}^{n_0} Q_{d_i}^s\frac{V_i^{\alpha-1}}{V_i^{s\alpha}}\frac{\partial V_i}{\partial t_{cl}} - \sum_{i=1}^{n-1}\sum_{j=i+1}^{n} B_{ij}(V_j\cos\theta_{ij}\frac{\partial V_i}{\partial t_{cl}} + V_i\cos\theta_{ij}\frac{\partial V_j}{\partial t_{cl}} - V_iV_j\sin\theta_{ij}\frac{\partial \theta_{ij}}{\partial t_{cl}})
\end{aligned}
\tag{20}
$$

The partial derivatives of $\tilde{\omega}_{g_i}$, θ, and V with respect to t_{cl} are the sensitivities obtained by integrating the dynamic system and the sensitivity system as discussed earlier.

The sensitivity *S* = $\frac{\partial \nu}{\partial t_{cl}}$ is computed for two different values of t_{cl}, which are chosen to be less than t_{cr}. Since we are computing only first-order trajectory sensitivities, the two values of t_{cl} must be less than t_{cr} by at most 20%. This might appear to be a limitation of the method. However, extensive experience with the system generally will give us a good estimate of t_{cr}. Because the system under consideration is stable, the sensitivity *S* will display larger excursions for larger t_{cl} [9]. Since sensitivities generally increase rapidly with increases in t_{cl}, we plot the reciprocal of the maximum deviation of *S* over the postfault period as $\eta = \frac{1}{\max(S)-\min(S)}$. A straight line is then constructed through the two points (t_{cl1},η_1) and (t_{cl2},η_2). The estimated critical clearing time $t_{cr,est}$ is the intersection of the constructed straight line with the time-axis in the (t_{cl},η)-plane as shown in Fig 2. As discussed later, this linearity is valid for a small region around t_{cr}.

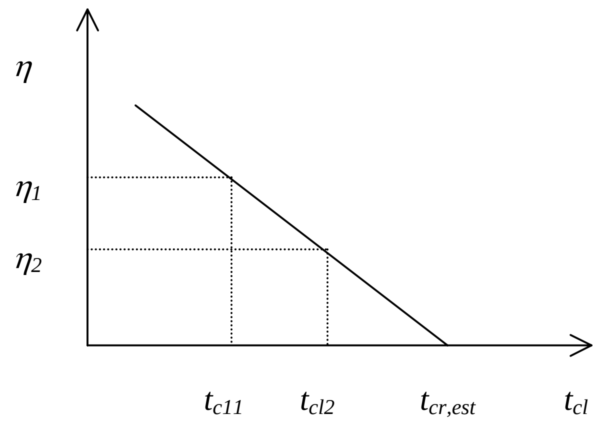

Fig. 2. Estimate of t_{cr}

Direct Use of Trajectory Sensitivities to Compute Critical Clearing Time [22]

In this section we outline an approach using trajectory sensitivity information *directly* instead of via the energy function to estimate the critical clearing time. To motivate this approach, let us consider a SMIB system described by

$$\begin{array}{ll} M\ddot{\delta} + D\dot{\delta} = P_M & 0 < t \le t_{cl} \\ M\ddot{\delta} + D\dot{\delta} = P_M - P_{em}\sin\delta & t > t_{cl} \end{array}, \ \delta(0) = \delta_0, \ \dot{\delta}(0) = 0 \tag{21}$$

The corresponding sensitivity equations are

$$\begin{array}{ll} M\ddot{u} + D\dot{u} = 0 & 0 < t \le t_{cl} \\ M\ddot{u} + D\dot{u} = (-P_{em}\cos\delta)u & t > t_{cl} \end{array}, \ u(0) = 0, \ \dot{u}(0) = 0 \tag{22}$$

where $u = \dfrac{\partial\delta}{\partial t_{cl}}$.

If we plot the phase plane portrait of the system for two values of t_{cl}, one small and the other close to t_{cr} and monitor the behavior of sensitivities in the $(u, \dot{u})$-plane we observe that the sensitivity magnitudes increase much more rapidly as t_{cl} approaches t_{cr}. Also, the trajectories in the $(u, \dot{u})$-plane can cross each other since the system (22) is time varying, whereas that is not the case for the system (21), which is an autonomous system. Qualitatively, both trajectories in the (δ, ω) -plane and the $(u, \dot{u})$-plane give the same information about the stability of the system, but the sensitivities seem to be stronger indicators because of their rapid changes in magnitude as t_{cl} increases. Hence, we can associate sensitivity information with the stability level of the system for a particular clearing time. When the system is very close to instability, the sensitivity reflects this situation much more quickly. This qualitative relationship has been discussed for the general nonlinear dynamic systems by Tomovic [15]. One possible measure of proximity to instability may be through some norm of the sensitivity vector. The Euclidean norm is one such possibility. For the single machine system, if we plot the norm $\sqrt{u^2 + \dot{u}^2}$ as a function of time for different values of t_{cl}, one can get a quick idea about the system stability as shown in Figs. 3 and 4. For a stable system, although the sensitivity norm tends to become a small value eventually, it transiently assumes a very high value when t_{cl} is close to t_{cr}.

Thus, we associate with each value of t_{cl} the maximum value of the sensitivity norm. The procedure to calculate the estimated value of t_{cr} is the same as described in the previous section but using the sensitivity norm instead of the energy function sensitivity. Here, the sensitivity norm for an *m*-machine system is defined as

$$S_N = \sqrt{\sum_{i=1}^{m}\left(\left(\frac{\partial \delta_i}{\partial t_{cl}} - \frac{\partial \delta_j}{\partial t_{cl}}\right)^2 + \left(\frac{\partial \omega_i}{\partial t_{cl}}\right)^2\right)}$$

where the *j*th-machine is chosen as the reference machine.

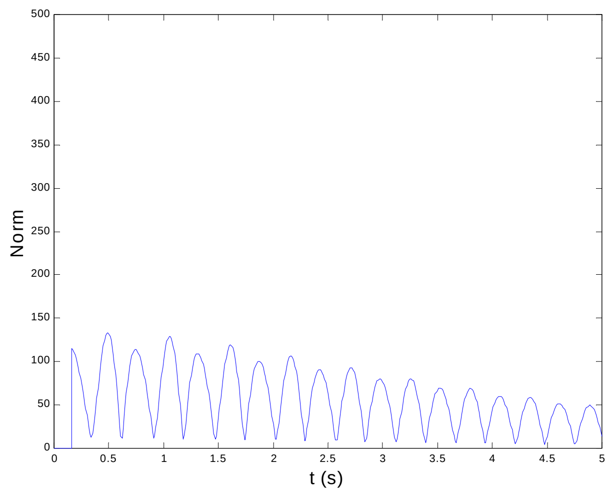

Fig. 3. Sensitivity norm for small t_{cl} ($\approx$ 50% of t_{cr})

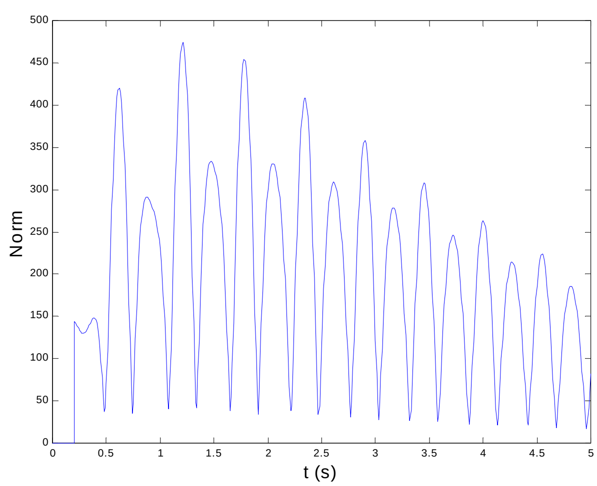

Fig. 4. Sensitivity norm for t_{cl} close to t_{cr} ($\approx$ 80% of t_{cr})

The norm is calculated for two values of $t_{cl} < t_{cr}$. For each t_{cl}, the reciprocal η of the maximum of the norm is calculated. A line through these two values of η is then extrapolated to obtain the estimated value of t_{cr}. If other parameters of interest are chosen instead, the technique will give an estimate of critical values of those parameters.

Since this technique does not require computation of the energy function, it can be applied to power systems without any restriction on system modeling. This is a major advantage of this technique.

Numerical Examples

We consider three systems and application of both energy function based and direct sensitivity based metric. These are the 3-machine, 9-bus [23, 24]; the 10-machine, 39-bus [3]; and the 50-machine, 145-bus [4] systems. Results are presented in Tables 1-2 and Fig. 5.

Table 1. Results for the 3-machine system

Faulted Bus	TEF Sensitivity	Sensitivity Norm	Actual
	$t_{cr,est}$ (s)	$t_{cr,est}$ (s)	t_{cr} (s)
5	0.354	0.352	0.352
8	0.333	0.333	0.334

Table 2. Results for the 10-machine system

Faulted bus	Line Tripped	Sensitivity Norm	Actual
		$t_{cr,est}$ (s)	t_{cr} (s)
4	4-5	0.210	0.212
15	15-16	0.204	0.206
17	17-18	0.169	0.168
21	21-22	0.122	0.125

For the 50-machine system, the estimated value of clearing time for a self-clearing fault at bus 58 using the sensitivity norm technique is computed. The corresponding values of η for different values of t_{cl} are shown in Fig. 5. We note that from Fig. 5 that if the two values of t_{cl} are chosen in the close range of t_{cr} = 0.315 s, the estimated value of t_{cr} will be quite accurate. On the other hand, picking arbitrary values of t_{cl} may give erroneous results. Since computing sensitivities is computationally extensive, choosing good values of t_{cl} requires judgment and experience.

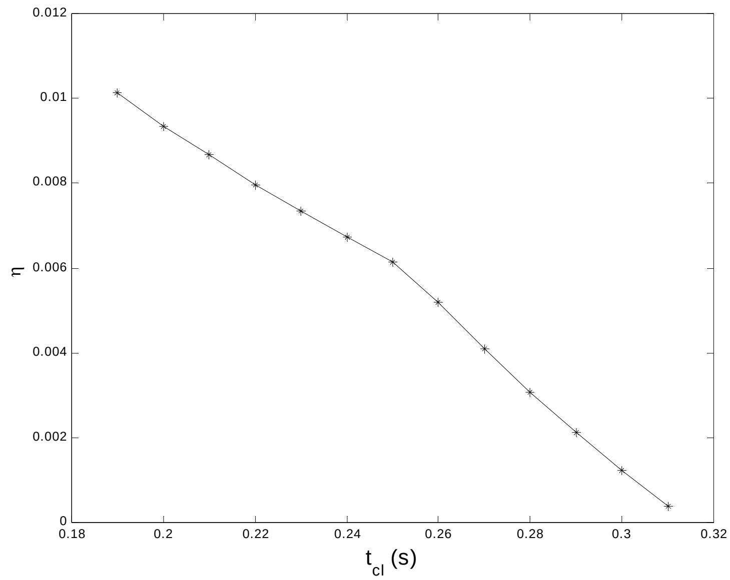

Fig. 5. Estimate t_{cr} for fault at bus 58 using norm sensitivity

Computation of Critical Loading of Generator

Next, the sensitivity norm technique is used to estimate the critical value of generator loading, or equivalently, the mechanical input power P_M. Two simulations for two values of P_M are carried out. The change from normal operating values in P_M is distributed uniformly among all loads in the system, so that the loading of the rest of the generators is unchanged. The sensitivity norm is calculated for the two specified values of P_M and then extrapolated to obtain the estimated value of the critical P_M for the chosen generator.

The 10-machine system

A fault is simulated in the system at bus 21 of the 10-machine system and cleared at $t_{cl} = 0.1$ s by tripping the line 21-22. The estimated results for a few generators are shown in Table 3.

Table 3. Estimated value of critical input power P_M vs. the actual value

Machine Number	Sensitivity Norm	Actual
	$P_{Mcr,est}$ (pu)	$P_{M,cr}$ (pu)
3	10.7	10.4
5	6.3	6.4
8	12.4	12.2

The 50-machine system

A self-clearing fault is simulated at bus 58 and cleared at t_{cl} = 0.15 s. Applying the proposed technique, the results obtained for critical value of P_M is and shown in Table 4. To validate the results it was verified that with the critical value of P_M the system goes unstable.

Table 4. Estimated value of critical input power P_M vs. the actual value

Machine Number	Sensitivity Norm	Actual
	$P_{M,est}$ (pu)	$P_{M,act}$ (pu)
4	22.9	22.3
5	17.0	16.5
7	4.3	4.2
12	10.0	9.6

Computation of Critical Impedance of a Transmission Line

The norm sensitivity technique is used to estimate the critical value of a line reactance. The 3-machine system is used to illustrate the technique. A fault is simulated at bus 7 and cleared at t_{cl} = 0.08 s by tripping the line 5-7. Figure 6 shows the corresponding values of η for different values of reactance of the line 8-9. The critical value of the reactance of line 8-9 is 0.246 pu. It can be seen from Fig. 6 that the estimated value of the critical reactance is quite accurate if the two values of the line reactance are picked in the close range of the actual critical value.

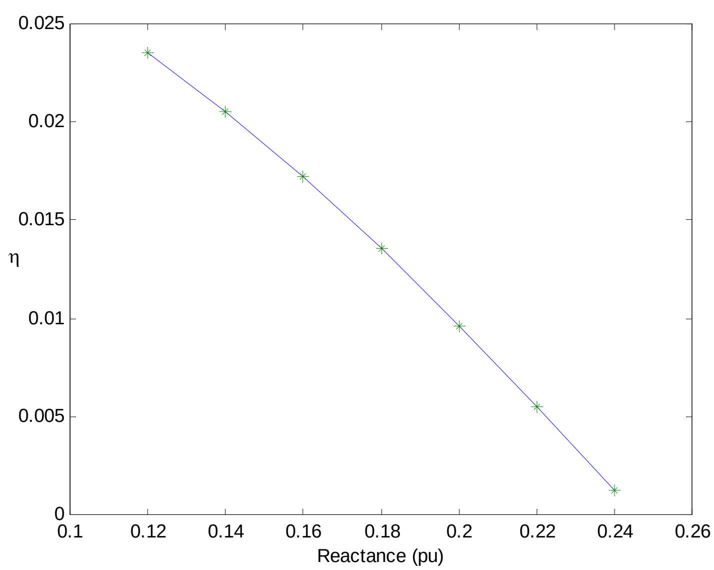

Fig.6. Estimate critical value of the reactance of the line 8-9

Knowing the critical value of a line reactance is very important in controlling power flow path in the system by the variable impedance devices. Such devices belong to a type of devices called flexible ac transmission systems (FACTS) that can be very useful in controlling the stability of power systems [25].

4. Stability Constrained Optimal Power Flow Formulation [10]

While Ref [26] formulates the problem in a different way, here we use the relative rotor angles to detect the system stability/instability of the power system. To check the stability of the system for a credible contingency, relative rotor angles are monitored at each time step during dynamic simulation. The sensitivities are also computed at the same time. Although sensitivity computation requires extensive computational effort, efficient method to compute sensitivities is available by making effective use of the Jacobian which is common to both the system and sensitivity equations [27]. This will reduce the computational burden considerably. We propose that when the relative rotor angle $\delta_{ij} = \delta_i - \delta_j > \pi$ for a given contingency, the system is considered as unstable. This is an extreme case as pointed out in [6], and one can choose an angle difference less than π depending on the system. Here *i* and *j* refer to the most and the least advanced generators respectively. The sensitivities of the rotor angles at this instant are used to compute the amount of power needed to be shifted from the most advanced generator (generator *i*) to the least advanced one (generator *j*) according to the formulae

$$\Delta P_{i,j} = \left. \frac{\delta_{ij} - \delta_{ij}^0}{\frac{\partial \delta_{ij}}{\partial P_i}} \right|_{\max \delta_{ij} = \pi} \tag{23}$$

$$P_i^{new} = P_i^0 - \Delta P_{i,j} \quad \text{and} \quad P_j^{new} = P_j^0 + \Delta P_{i,j} \tag{24}$$

where P_i^0, P_j^0, and δ_{ij}^0 are the base loading of generators *i* and *j*, and the relative rotor angle of the two respectively at the solution of the OPF problem. $\frac{\partial \delta_{ij}}{\partial P_i}$ is the sensitivity of relative rotor angle with respect to the output of the *i*th-generator; P_i in this case is the parameter λ in equations stated in Section 3.

After shifting the power from generator *i* to generator *j* according to (24), the system is secure for that contingency but it is not an optimal schedule. We can improve the optimality by introducing new power constraints on generation. The OPF problem with new constraints is then re-solved to obtain the new operating point for the system. The detailed algorithm is discussed in [10]

5. Assessment of Transmission Protection System Vulnerability to Angle Stability Problems

Power system protection at the transmission system level is based on distance relaying. Distance relaying serves the dual purpose of apparatus protection and system protection. Significant power flow oscillations can occur on a transmission line or a network due to major disturbances like faults and subsequent clearing, load rejection, etc. They are related to the swings in the rotor angles of synchronous generators. If the rotor angles settle down to a new stable equilibrium point, the disturbance is classified as stable. Otherwise, it is unstable. Hence, for stable disturbances, power swings die down with time.

In this section, we discuss the application of trajectory sensitivity analysis to detect vulnerable relays in the system. For each contingency we compute a quantity called branch impedance sensitivity, which will be used to identify weak links in the system. Its main advantage is that it can handle systems of any degree of complexity in terms of modeling and can be used as an on-line DSA tool.

Distance relays are used to detect swings and take appropriate action (tripping or blocking) depending on the nature of swing (stable or unstable). The reason is that a change in transmission line power flow translates into a corresponding change in the impedance seen by the relay. Relay operation after fault clearing depends upon the power swing and proximity of the relay to an electrical center.

The apparent impedance seen by a relay on a transmission line connecting nodes *i* and *j* having flow $P_{ij} + jQ_{ij}$ is given by

$$Z_{app} = \left[\frac{P_{ij}}{P_{ij}^2 + Q_{ij}^2} + j\frac{Q_{ij}}{P_{ij}^2 + Q_{ij}^2} \right] |V_i|^2 \tag{25}$$

As $|V_i|$ is only a scalar, it cannot differentiate between the quadrants in the *R*-*X* plane. Thus, the location of Z_{app} depends on the direction of *P* and *Q* flows. Clearly, swings are severe when P_{ij} and/or Q_{ij} are large and V_i small. Under such circumstance Z_{app} is small, and hence can cause a relay to trip.

Work based upon Lyapunov stability criterion has been reported in [28] to rank relays according to the severity of swings. In [29] relay margin is used as a measure of how close a relay is from issuing a trip command. Basically, it is the ratio of the time of longest consecutive stay of a swing in zone to its time dial setting (TDS). For relays that see swing characteristic outside of their zone settings, the relay space margin is used. It is defined as the smallest distance between the relay characteristic and the swing trajectory in *R*-*X* plane. To identify the most vulnerable relay, magnitude of the ratio of swing impedance to line impedance is used as a performance parameter. The most vulnerable relay corresponds to one with minimum ratio, where the search space extends over all the relays and time instants of simulation.

Reference [30] discusses the challenges to relaying in the restructured power system operation scenario. In such a scenario, there will be varying power flow patterns dictated by the market conditions. During the congestion period, relay margins and relay space margins will be reduced. This may pose challenges to system protection design.

The vulnerability of a relay to power swings is directly dependent on severity of oscillations in power flow observed in the primary transmission line and adjacent transmission lines that are covered by backup zones. Hence, the problem of assessment of transmission protection system vulnerability to power swings translates into assessment of oscillations in power flow on a transmission system due to disturbance.

We will show that branch impedance trajectory sensitivity (BITS) (that is, trajectory sensitivity of rotor angles to branch impedance), can be used to locate electrical center [9] in the transmission system and rank transmission system distance relays according to their vulnerability to tripping on swings.

Electrical center and weakest link in a network

For power systems that essentially behave as a two-area system under instability, the out-of-step relaying can be explained by considering the equivalent generators connected by a tie line. When the two generators fall out of step, i.e., the angular difference between the two generator voltage phasors is 180°, they create a voltage zero point on the connecting circuit. This is known as the electrical center. A distance relay perceives it as a solid 3-phase short-circuit and trips the line.

One way to locate the electrical center [31] in a power system is to create a fault with fault clearing time greater than the critical clearing time of the circuit breaker to make the resulting postfault system unstable. Through transient stability simulations, one identifies the groups of accelerating and decelerating machines in the system. The sub network interconnecting such groups will contain the electrical center. For the relays contained in the sub network, by simulating the power swing on the *R-X* plane one can locate the relays for which the power swing intersects the transmission line impedance. This line contains the electrical center of the system. The electrical center will also be observed by the backup relays depending upon their zone 2 and 3 setting. Usually, the relays near the electrical center are highly sensitive to power swings. A well-known property to characterize an electrical center is that the network adjoining the electrical center has low voltages. Such characterization is qualitative and can be used as a screening tool. Since natural splitting of the system due to operation of distance relays takes place at the electrical center, we refer to such a line (or a transformer) as the weakest link in the network.

To compress the information of all rotor angles with respect to a given line, for an *m*-machine system the following norm first introduced in [22] is used in the numerical examples section. The BITS norm is computed as follows:

$$S_N = \sqrt{\sum_{i=1}^{m}\left(\frac{\partial \alpha_i}{\partial x}\right)^2 + \sum_{i=1}^{m}\left(\frac{\partial \omega_i}{\partial x}\right)^2} \tag{26}$$

where $\alpha_i = \delta_i - \delta_j$ and the *j*th-machine is chosen as the reference, and *x* is the transmission line reactance.

Numerical Examples

A 10-machine, 39-bus system [3] is used for illustrative examples. The following two cases are considered.

Fault at bus 28

The fault is cleared at t_{cl} = 0.06 s by tripping line 28-29 simultaneously from both ends. Table 5 captures the normalized indices for a subset of lines, which have high, medium, and low sensitivities. BITS sensitivity norm is computed for all the lines and normalized with respect to the maximum one. Therefore, after normalization, the line with max BITS norm has value 1. For all other lines, BITS norm is less than or equal to 1. We would characterize the line 29-26 as the most vulnerable line because its rank is 1, and its absolute peak norm of 30 822 is also very high. The normalized indices for all other lines are much lower than that of the line 29-26. Hence, other lines are less vulnerable to the swing. These inferences have been confirmed by using the relay space margin (RSM) concept. Figures 6 and 7 show the swing curves for relay on lines 29-26 and 26-27 respectively.

Table 5. Normalized BITS norm (nominal or 100 % loading)

Line	Normalized Sensitivity	RSM	$\lvert Z_{min} \rvert$
29-26	1	0.0231	0.0658
26-27	0.1630	0.1759	0.1841
26-25	0.1511	0.1870	0.2578
26-28	0.0111	0.4842	0.5077

As line 29-26 is the weakest link in the post fault system, it has a large possibility of developing the electrical center in case a fault leads to instability (because of larger t_{cl} or system loadings). To confirm the location of the electrical center, t_{cl} was increased from 0.06 s to 0.07 s to create system instability. The small increase of 0.01 s in fault clearing time induced instability. This indicates that existing system is working close to its stability limits.

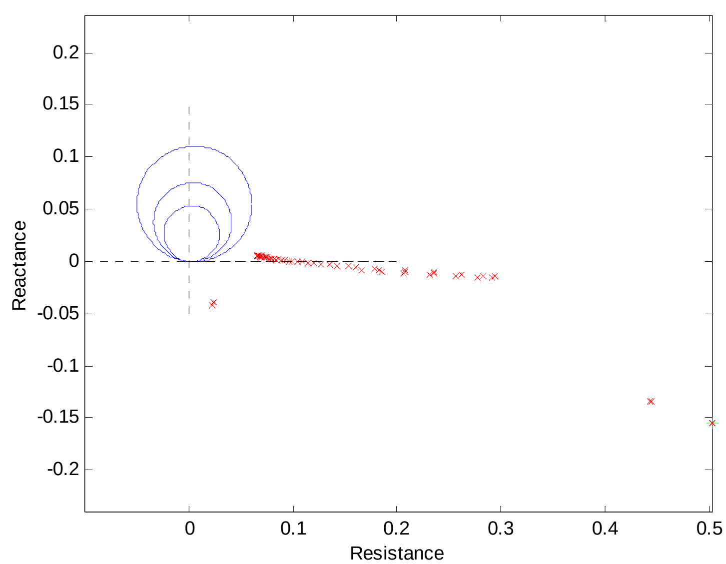

Fig. 6. Swing curve for relay on line 29-26 (stable)

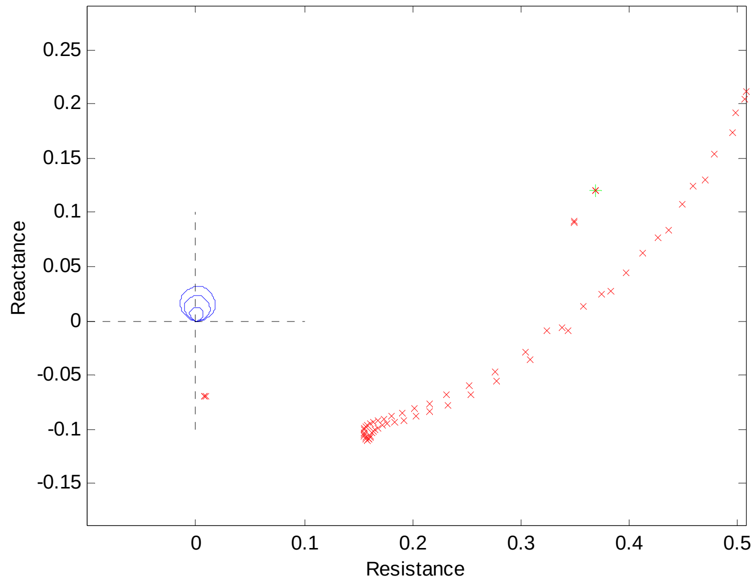

Fig. 7. Swing curve for relay on line 26-27 (stable)

The swing trajectory for the relay on line 29-26 located near bus 29 for $t_{cl} = 0.07$ s is shown in Fig. 8. As the trajectory cuts the transmission line characteristic in zone 1, the location of electrical center on 29-26 is thus established. This is clearly an unstable case. The relative rotor angles in this case are show in Fig. 9 where machine 9 is the unstable machine.

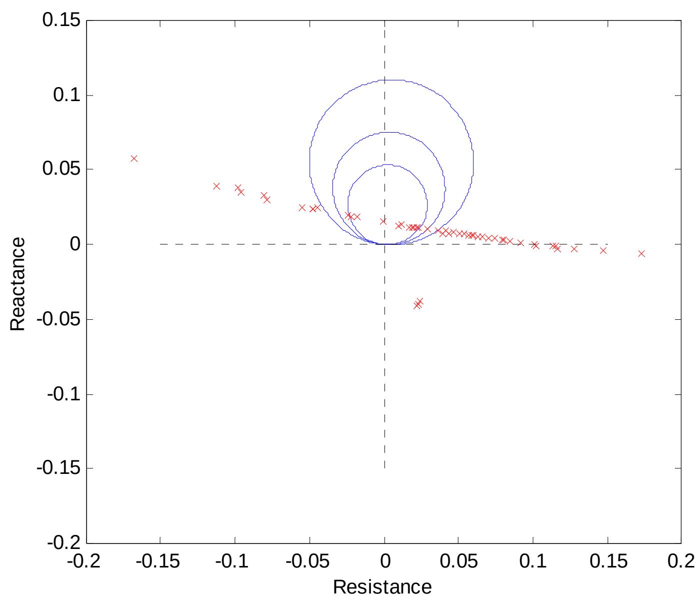

Fig. 8. Electrical center location on line 29-26 (unstable)

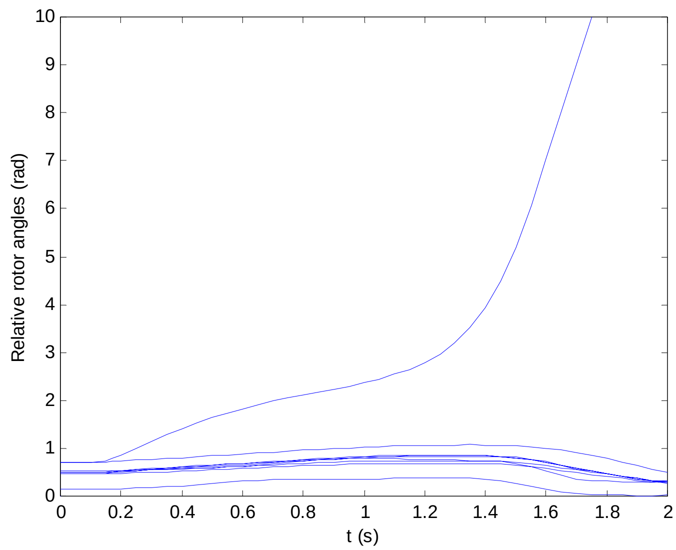

Fig. 9. Relative rotor angles for the unstable case

Table 6 summarizes actual BITS norms as well as the results for various loading conditions (80%, 90%, and 100% of the system load). It can be seen that as system loading increases, the trajectory sensitivity also increases. As the system approaches a dynamical stability limit, the trajectory sensitivity for the critical line jumps from 145.17 for 90 % loading case to 30 822 for 100 % loading case. Thus, a high peak value of maximum sensitivity can be used as an indicator of reduced stability margins. Also, note that the sensitivity norm changes rapidly when the system loading approaches the stability boundary. Therefore, it can be used as an indicator for system stability margin.

Table 6. Absolute norm for different loading conditions

Line	80% load	90% load	100% load
29-26	90.2730	145.1799	30822
26-27	25.6782	31.7447	5022
26-25	9.4081	20.0233	4656
26-28	5.8828	6.8147	343.09

Fault at bus 4

The fault is cleared at t_{cl} = 0.1 s by tripping line 4-5 simultaneously from both ends. For this scenario, results similar to the case discussed earlier are summarized in Tables 7 and 8. Electrical center is located on line 1-2. The results replicate the same pattern of behavior as discussed in the previous case. From Table 8 it can be seen that peak sensitivity norm is quite low (60 in comparison to 30 822 of Table 6), and the sensitivity norm does not change much with various loading conditions. It indicates that for this fault, the loading conditions are such that the system is still far away from the stability boundary. In fact, the critical clearing time for this fault with the nominal loading condition is 0.29 s.

Table 7. Normalized BITS norm with 100 % load

Line	Normalized sensitivity	RSM	$\lvert Z_{min} \rvert$
1-2	1	0.1600	0.1900
1-39	0.9680	0.1694	0.2036
2-25	0.6196	0.2337	0.2036
14-15	0.5409	0.3201	0.3310

Table 8. Absolute BITS norm for various loading conditions

Line	90% load	100% load	110% load
1-2	53.7342	57.4645	60.6352
1-39	51.1508	55.6236	58.0612
2-25	29.1845	35.6055	53.0692
14-15	26.5545	31.0798	36.3755

This section has developed the concept of maximum rotor angle branch impedance trajectory sensitivity as a tool for assessing transmission protection system vulnerability to angle stability problems. It is used for applications in power systems such as

i. Ranking transmission lines and relays as vulnerability to swings. The ranking can help to improve the relay coordination in the presence of power swings.
ii. Determining location of electrical center. Because transmission lines adjoining the electrical center have low voltages, other devices such as FACTS could be used to strengthen system stability.
iii. Indicating stability margin. When BITS is getting higher, it indicates that the operating point of system is moving closer to the system stability boundary.

6. Conclusions

This paper summarizes a recent approach taken for dynamic security assessment of power systems using trajectory sensitivity analysis. It is independent of model complexity and requires some apriori knowledge of the system criticality. In power systems, years of experience provide this. Future research will involve applying this technique to relieve congestion in deregulated systems.

Future research should extend the application to exploring the connection between stability and sensitivity theory in hybrid dynamical systems which is an emerging area of research in control [32].

In power systems, examples include state dependent variation of taps in tap changing transformers or switching of FACTS devices for which the theory of trajectory sensitivity analysis is already available [21].

7. Acknowledgements

This research was supported by NSF grant ECS 00-00474 and the Grainger Foundation.

References

[1] G. L. Wilson and P. Zarakas, "Anatomy of a blackout," *IEEE Spectrum*, vol. 15, no. 2, pp. 38-46, Feb.1978.

[2] O. Alsac and B. Stott, "Optimal load flow with steady state security," *IEEE Transactions on Power Apparatus and Systems*, vol. PAS-93, pp. 745-754, 1974.

[3] M. A. Pai, *Energy Function Analysis for Power System Stability*. Norwell, MA: Kluwer Academic Publishers, 1989.

[4] A. A. Fouad and V. Vittal, *Power System Transient Stability Analysis Using the Transient Energy Function Method*. Englewood Cliffs, NJ: Prentice-Hall, 1991.

[5] H. D. Chiang, C. C. Chu, and G. Cauley, "Direct stability analysis of electric power system using energy functions: Theory, applications, and perspective," *Proceedings of the IEEE*, vol. 83, no. 11, pp. 1497-1529, Nov. 1995

[6] M. Pavella, D. Ernst, and D. Ruiz-Vega, *Transient Stability of Power Systems: A Unified Approach to Assessment and Control*. Norwell, MA: Kluwer Academic Publishers, 2000.

[7] K. W. Chan, A. R. Edwards, R.W. Dunn, and A. R. Daniels, "On-line dynamic security contingency screening using artificial neural networks," *IEE Proceddings on Generation, Transmission, and Distribution*, vol. 147, no. 6, pp. 367-372, Nov. 2000.

[8] Y. Mansour, E. Vaahedi, and M. A. El-Sharkawi, "Dynamic security contingency screening and ranking using neural networks," *IEEE Transactions on Neural Networks*, vol. 8, no. 4, pp. 942-950, July 1997.

[9] T. B. Nguyen, "Dynamic security assessment of power systems using trajectory sensitivity approach," Ph.D. dissertation, University of Illinois, Urbana-Champaign, 2002.

[10] T. B. Nguyen and M. A. Pai, "Dynamic security-constrained rescheduling of power systems using trajectory sensitivities," *IEEE Transactions on Power Systems*, to appear.

[11] H. You, V. Vittal, Z. Yang, "Self-Healing in Power Systems: An approach using islanding and rate of frequency decline based load shedding," *IEEE Transactions on Power Systems*, to appear.

[12] P M. Frank, *Introduction to System Sensitivity Theory*. New York: Academic Press, 1978.

[13] M. Eslami, *Theory of Sensitivity in Dynamic Systems*. New York: Springer-Verlag,1994.

[14] H.. W. Bode, *Network Analysis and Feedback Amplifier Design*. New York: Van H Nostrand, 1945.

[15] R. Tomovic, *Sensitivity Analysis of Dynamic Systems*. New York: McGraw-Hill, 1963.

[16] R. Tomovic and M. Vukobratovic, *General Sensitivity Theory*. New York: American Elsevier, 1972.

[17] J. B. Cruz, Jr, Ed., *System Sensitivity Analysis*. Stroudsburg, PA: Dowden, Hutchingson and Ross, 1973.

[18] G. C. Verghese, I. J. Perez-Arriaga, and F. C. Scheweppe, “Selective modal analysis with applications to electric power systems, Part I and II,” *IEEE Transactions on Power Apparatus and Systems*, PAS-101, pp. 3117-3134, Sep. 1982.

[19] M. J. Laufenberg and M. A. Pai, “A new approach to dynamic security assessment using trajectory sensitivities,” *IEEE Transactions on Power Systems*, vol. 13, no. 3, pp. 953-958, Aug. 1998.

[20] I. A. Hiskens and M. Akke, “Analysis of the Nordel power gird disturbance of January 1, 1997 using trajectory sensitivities,” *IEEE Transactions on Power Systems*, vol. 14, no. 3, pp. 987-994, Aug. 1999.

[21] I. A. Hiskens and M. A. Pai, “Trajectory sensitivity analysis of hybrid systems,” *IEEE Transactions on Circuits and Systems Part I: Fundamental Theory and Applications*, vol. 47, no. 2, pp. 204-220, Feb. 2000.

[22] T. B. Nguyen, M. A. Pai, and I. A. Hiskens, “Sensitivity approaches for direct computation of critical parameters in a power system,” *International Journal of Electrical Power and Energy Systems*, vol. 24, no. 5, pp. 337-343, 2002.

[23] P. W. Sauer and M. A. Pai, *Power System Dynamics and Stability*. Upper Saddle River, NJ: Prentice-Hall, 1998.

[24] K. R. Padiyar, *Power System Dynamics Stability and Control*. B.S Publications, Hyderabad, India, 2002.

[25] N. G. Hingorani and L. GyuGyi, *Understanding FACTS Concepts and Technology of Flexible AC Transmission Systems.* New York: IEEE Press, 2000.

[26] D. Gan, R. J. Thomas, and R. Zimmerman, “Stability-constrained optimal power flow,” *IEEE Transactions on Power Systems*, vol. 15, pp. 535-540, May 2000.

[27] D. Chaniotis, M. A. Pai, and I. A. Hiskens, “Sensitivity analysis of differential-algebraic systems using the GMRES method – Application to power systems,” *Proceedings of the IEEE International Symposium on Circuits and Systems*, Sydney, Australia, May 2001.

[28] C. Singh and I. A. Hiskens, “Direct assessment of protection operation and non-viable transients,” *IEEE Transactions on Power Systems*, vol. 16, no. 3, pp. 427-434, Aug. 2001.

[29] F. Dobraca, M. A. Pai, and P. W. Sauer, “Relay margins as a tool for dynamical security analysis,” *International Journal of Electrical Power and Energy Systems*, vol. 12, no. 4, pp. 226-234, Oct. 1990.

[30] J. S. Thorp and A. G. Phadke, “Protecting power systems in the post-restructuring era,” *IEEE Computer Applications in Power*, vol. 12, no. 1, pp. 33-37, Jan. 1999.

[31] P. Kundur, *Power System Stability and Control*. New York: McGraw-Hill, 1994.

[32] A. N. Michel and B. Hu, “Toward a stability theory of general hybrid dynamical systems,” *Automatica*, vol. 35, pp. 371-384, 1999.